AMERICAN SOCIETY FOR MICROBIOLOGY | Journal of Virology

Virology | Full-Length Text

Degradation of TRIM32 is induced by RTA for Kaposi's sarcoma-associated herpesvirus lytic replication

Yulin Zhang,[1] Zhongwei Dong,[1] Feng Gu,[1] Yifei Xu,[1] Ying Li,[1] Wen Sun,[1] Wutian Rao,[1] Shujuan Du,[1] Caixia Zhu,[1] Yuyan Wang,[1] Fang Wei,[2] Qiliang Cai[1]

AUTHOR AFFILIATIONS See affiliation list on p. 17.

ABSTRACT TRIM32 is often aberrantly expressed in many types of cancers. Kaposi's sarcoma-associated herpesvirus (KSHV) is linked with several human malignancies, including Kaposi's sarcoma and primary effusion lymphomas (PELs). Increasing evidence has demonstrated the crucial role of KSHV lytic replication in viral tumorigenesis. However, the role of TRIM32 in herpesvirus lytic replication remains unclear. Here, we reveal that the expression of TRIM32 is upregulated by KSHV in latency, and reactivation of KSHV lytic replication leads to the inhibition of TRIM32 in PEL cells. Strikingly, RTA, the master regulator of lytic replication, interacts with TRIM32 and dramatically promotes TRIM32 for degradation via the proteasome systems. Inhibition of TRIM32 induces cell apoptosis and in turn inhibits the proliferation and colony formation of KSHV-infected PEL cells and facilitates the reactivation of KSHV lytic replication and virion production. Thus, our data imply that the degradation of TRIM32 is vital for the lytic activation of KSHV and is a potential therapeutic target for KSHV-associated cancers.

IMPORTANCE TRIM32 is associated with many cancers and viral infections; however, the role of TRIM32 in viral oncogenesis remains largely unknown. In this study, we found that the expression of TRIM32 is elevated by Kaposi's sarcoma-associated herpesvirus (KSHV) in latency, and RTA (the master regulator of lytic replication) induces TRIM32 for proteasome degradation upon viral lytic reactivation. This finding provides a potential therapeutic target for KSHV-associated cancers.

KEYWORDS TRIM32, KSHV, RTA, lytic replication

The tripartite motif (TRIM) family proteins, the majority of which possess E3 ubiquitin ligase activities, exhibit multiple functionalities in cellular processes encompassing intracellular signaling, developmental pathways, apoptosis regulation, innate immunity responses, autophagy modulation, and carcinogenesis progression (1). TRIM proteins are characterized by an N-terminal region consisting of one RING finger domain and one or two zinc finger domains known as B box (B1- and B2-box) (2, 3), along with their associated coiled-coil region (4). Most of the TRIM family proteins have the activities of E3 ubiquitin ligases due to containing a RING finger domain (5–7). TRIM proteins possess a diverse domain at the carboxyl terminus, including the domains of SPRY, NHL, and PHD (1, 8). To date, more than 80 known TRIM proteins are classified in 11 subfamilies, according to the presence of C-terminal domains and one uncategorized group without the RING domain (8).

TRIM32, an important member of the TRIM family, has been identified as a pivotal player in the degradation process of diverse substrate proteins, including dysbindin, PIASy, and Abl-2 (9), and extensively implicated in many diseases, including malignancies and viral infections (10, 11). Interestingly, TRIM32 is aberrantly expressed in many cancers, including head and neck squamous cell carcinoma, colorectal cancer,

Editor Jae U. Jung, Lerner Research Institute, Cleveland Clinic, Cleveland, Ohio, USA

Address correspondence to Qiliang Cai, qiliang@fudan.edu.cn, Fang Wei, fangwei@sjtu.edu.cn, or Yuyan Wang, yuyanss@fudan.edu.cn.

Yulin Zhang, Zhongwei Dong, Feng Gu, Yifei Xu, and Ying Li contributed equally to this article. Author order was determined both alphabetically and in order of increasing seniority.

The authors declare no conflict of interest.

See the funding table on p. 18.

Received 3 January 2024
Accepted 5 April 2024
Published 8 May 2024

hepatocellular carcinoma, and lung cancer (12–14). It has been shown that TRIM32 not only enhances TNFα-mediated apoptosis via XIAP degradation, thereby augmenting tumor cell sensitivity to chemotherapeutic agents (15–17), but also is potentially involved in antiviral infection (18, 19) and immune regulation (18, 20) by its ubiquitin-protein ligase activity (21). For example, TRIM32 can directly induce K63-linked polyubiquitination of STING upon cytosolic DNA stimulation to facilitate the induction of an antiviral response (22) and can negatively regulate TLR3/4-mediated immune responses (23). These findings suggest that regulating TRIM32 expression may be indispensable for preserving cell growth and viral infection.

Kaposi's sarcoma-associated herpesvirus (KSHV), also known as human herpesvirus 8 (HHV-8), is an oncogenic γ-herpesvirus and highly homologous with Epstein–Barr virus. KSHV has been documented as the etiological agent for Kaposi's sarcoma (KS), primary effusion lymphoma (PEL), and the plasma cell variant of multicentric Castleman disease (24, 25). Like other herpesviruses, KSHV is capable of establishing latent infection in host cells and reactivating for lytic replication under certain conditions (26). Although the majority of KSHV-positive cells in cancer are in a latent state of infection, approximately 1%–3% of the cells exhibit a lytic state of virus activation (27). Increasing evidence has shown that the sequential expression of viral lytic products (immediate early, early, and late genes) may promote cell proliferation, angiogenesis, and local inflammation, leading to the initiation and progression of KS tumors (28–32). The majority of the KSHV genome remains transcriptionally quiescent during latency; however, the expression of the lytic genes is essential and sufficient to trigger the transition from latent to lytic replication (33). The first lytic gene to be expressed during lytic cycle replication in B lymphocytes is the immediate early gene, *Rta* (ORF50) (33), which produces RTA serving as a viral transcription factor that controls the switch from the latent to the lytic cycle and triggers the expression of early genes including ORF59 (34, 35), followed by the expression of late genes (32, 36–38). In latently infected cells, RTA (as replication and transcription activator) expression is tightly restricted, indicating that the *Rta* gene is transcriptionally repressed in established latency host cells (39). The repression of RTA expression has been demonstrated to involve the regulation of numerous viral and cellular factors. RTA possesses the activity of a ubiquitin E3 ligase to target substrates for degradation selectively (40, 41).

In terms of the role of TRIM32 in herpesvirus infection and mediated pathogenesis, it has been reported that TRIM32 served as a crucial positive regulator of HSV-1-induced IFN-β production in corneal epithelial cells and played a predominant role in clearing HSV-1 from the cornea (42). A recent study showed that TRIM32 also causes STING to ubiquitinate at the Lys150 site, leading to the recruitment of VP1-1 for viral immune evasion (43). However, the role of TRIM32 in the regulation of KSHV life cycle remains unclear.

In this study, we found that the expression of TRIM32 was elevated in KSHV latently infected cells, and reactivation of KSHV lytic replication upon chemical stimulation leads to the inhibition of TRIM32 in PEL cells. Importantly, RTA, the master regulator of lytic reactivation, interacts with TRIM32 and promotes TRIM32 for proteasomal degradation. Knockdown of TRIM32 reduces the cell proliferation and colony formation of KSHV-infected PEL cells, which in turn facilitates the reactivation of KSHV lytic replication and virion production. Thus, our findings imply that the degradation of TRIM32 induced by RTA is important for the lytic activation of KSHV, which provides an attractive therapeutic target for KSHV-associated cancers.

RESULTS

Inhibition of TRIM32 contributes to the reactivation of KSHV lytic replication

It has been reported that TRIM32 is overexpressed in various tumor tissues (10). To explore whether the expression of TRIM32 is associated with KSHV-infected tumor cells, we first detected the protein levels of TRIM32 in KSHV latently infected PEL (BC1, BC3, BCBL1, and JSC1) and uninfected B-lymphoma (BJAB) cell lines by immunoblotting (IB)

assays. The results showed that the protein levels of TRIM32 were dramatically elevated in PEL cells, when compared with KSHV-uninfected BJAB cells (Fig. 1A). To confirm if the elevation of TRIM32 protein levels is due to KSHV infection during latency, we also detected the protein levels of TRIM32 in paired cell lines, including KSHV latently infected B-lymphoma BJAB (K-BAJB), epithelial iSLK (iSLK-Bac16), and rat endothelial MM (KMM) cell lines, and their uninfected parental cell lines (BJAB, iSLK, and MM). Supportingly, the expression level of TRIM32 protein was consistently higher in KSHV-infected cells (K-BJAB, KMM, and iSLK-16) than in the KSHV-negative cells (BJAB, MM, and iSLK) (Fig. 1B). These data suggest that the TRIM32 protein level is increased in cells latently infected by KSHV.

To explore the role of TRIM32 in KSHV latent infection, BCBL1 cells stably transduced with a recombinant lentivirus expressing small hairpin RNA targeting TRIM32 (shTRIM32) or luciferase control (shCtrl) were first generated and assessed. The results of quantitative PCR showed a significant reduction in TRIM32 transcript in the shTRIM32 group, when compared with the shCtrl or parental mock group (Fig. 2A), which was further confirmed by the results of consistently lower protein levels by immunoblotting assays (Fig. 2B). Strikingly, we observed that the inhibition of TRIM32 expression dramatically led to an upregulation of RTA expression (Fig. 2B). Furthermore, subsequent quantitative PCR analysis revealed a significant increase in transcriptional expression of both immediately early gene ORF50 (RTA) and early gene ORF59 upon TRIM32 knockdown (Fig. 2C), indicating that TRIM32 is a key host molecule involved in the regulation of viral lytic replication. To further assess the impact of TRIM32 knockdown on the intracellular viral episome copy number, we also performed quantitative PCR to detect the viral genome copy number change in the BCBL1 cells with or without TRIM32 knockdown by tittering the latent gene ORF72 and terminal repeat (TR) as described previously (44, 45). As shown in Fig. 2D, the inhibition of TRIM32 significantly enhanced viral genome replication, which may facilitate the reactivation of KSHV lytic replication.

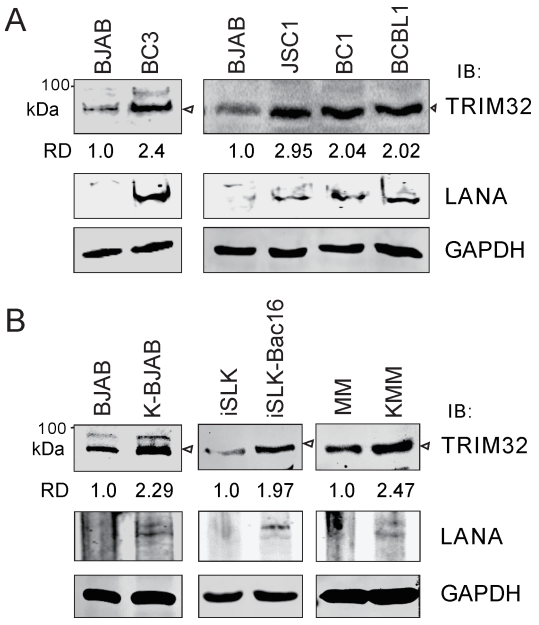

FIG 1 Expression of TRIM32 is elevated in KSHV latently infected cells. (A) High expression of TRIM32 in PEL cells. Equal numbers of KSHV-positive PEL (BC1, BC3, BCBL1, and JSC1) or negative BJAB cells were subjected to an immunoblotting assay with antibodies as indicated. (B) The expression of TRIM32 is elevated by KSHV in latent infection. Equal amounts of KSHV latently infected (K-BJAB, KMM, and iSLK-16) and its parental uninfected (BJAB, MM, and iSLK) cells were subjected to an immunoblotting assay with antibodies as indicated. Relative density (RD) of protein level of TRIM32 is quantified and shown.

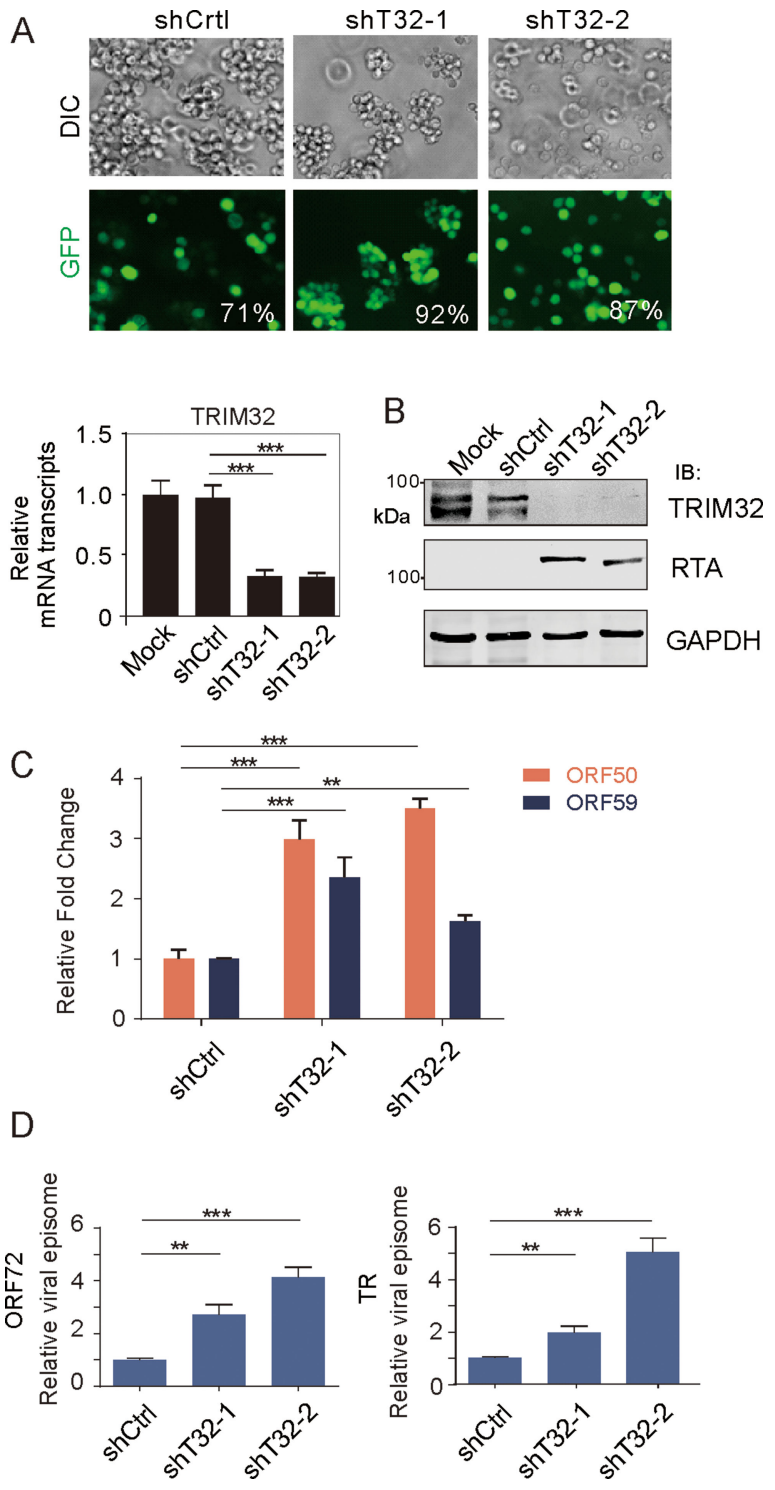

FIG 2 Inhibition of TRIM32 expression reactivates KSHV lytic replication and virion production. (A) Establishment of BCBL1 cells with TRIM32 knockdown. BCBL1 cells individually infected with lentivirus carrying green fluorescence protein (GFP)-tagged small hairpin RNA (shRNA) against TRIM32 (shT32-1 or shT32-2) or luciferase control (shCtrl) were analyzed by a fluorescence microscope (upper panel) or harvested for quantitative PCR (lower panel). Relative levels of TRIM32 transcripts are shown at the bottom panels. Uninfected cells were used as mock. The percentage of GFP-positive cells is quantified by flow cytometry and shown. DIC, differential interference contrast. (B) Knockdown of TRIM32 induces RTA

(Continued on next page)

FIG 2 (Continued)

expression in PEL cells. Whole cell lysates (WCLs) from BCBL1 cells with or without TRIM32 knockdown from panel (A) were individually subjected to an IB assay with antibodies as indicated in the figure. GAPDH was used as an internal control. (C) Knockdown of TRIM32 enhances the transcription of KSHV lytic genes. Total RNA extracted from panel (A) was individually subjected to reverse transcription and quantitative PCR analysis for transcriptions of KSHV lytic genes including ORF50 and ORF59. (D) Knockdown of TRIM32 enhances the viral episome DNA copy number. The KSHV episome DNA extracted from panel (A) was subjected to quantitative PCR analysis for ORF72 and TR copies. The statistical significance was evaluated, and $P < 0.01$ was indicated by two asterisks; $P < 0.001$ was indicated by three asterisks.

Expression of TRIM32 is reduced during the lytic cycle of KSHV

Given that TRIM32 knockdown leads to the reactivation of KSHV lytic replication in PEL cells, to determine whether the reactivation of the KSHV lytic cycle reduces the expression of TRIM32, we treated KSHV-positive PEL (BCBL1 and BC3) cells with tetradecanoyl phorbol acetate (TPA) and sodium butyrate to activate KSHV from latency to lytic replication for 24 h, followed by immunoblotting analysis of TRIM32 and RTA. With the KSHV-negative B-lymphoma BJAB and DG75 cells as parallel controls, a significant reduction of TRIM32 and marked upregulation of RTA were observed in both KSHV-positive BCBL1 and BC3 cells upon the reactivation of lytic replication. In contrast, no significant change occurs in the KSHV-negative BJAB and DG75 cells (Fig. 3A). To address whether the reduction of the protein level of TRIM32 upon lytic reactivation is due to the inhibition at the transcriptional level, the mRNA levels of TRIM32 and RTA in PEL cells treated with TPA and sodium butyrate were individually quantified by quantitative PCR analysis. The results showed that the transcription levels of TRIM32 were increased slightly instead of decreased in both BCBL1 and BC3 cells upon TPA and sodium butyrate treatment, albeit the transcription of RTA was dramatically increased (Fig. 3B). There was no significant change in TRIM32 transcripts in KSHV-negative cells (Fig. 3B). These data indicate that the reactivation of KSHV lytic replication reduces TRIM32 expression at the protein level, rather than the transcriptional level. To reduce the effect of genetic background differences, three cell lines, 293T-219, iSLK-219, and iSLK-Bac16 [in which RTA expression or KSHV whole genome is under doxycycline (Dox) induction individually], were used for the induction of RTA expression, followed immunoblotting with TRIM32. A similar phenomenon of a dose-dependent reduction of TRIM32 at the protein level along with the increased expression of RTA in all three cell lines was observed (Fig. 3C, upper panel). In contrast, the mRNA levels of TRIM32 were not significantly changed in both iSLK-Bac16 and 293T-219 cells upon reactivation, albeit a slight increase was observed in iSLK-219 cells (Fig. 3C, lower panel). The results suggest that RTA may exert an inhibitory effect on the regulation of TRIM32 at the protein levels instead of transcriptional levels. The difference of TRIM32 transcripts in iSLK-16 and iSLK-219 cells indicates that the regulation of TRIM32 upon reactivation of lytic replication in different viral systems could be varied.

RTA induces TRIM32 degradation via the proteasome

It has been reported that RTA could serve as a ubiquitin E3 ligase to induce different substrates, including STAT6, for degradation during KSHV lytic replication (41, 46, 47). To further validate whether RTA also participates in the downregulation of TRIM32 at the protein level, we examined the expression of TRIM32 in iSLK cells carrying doxycycline-induced RTA alone upon Dox induction for different time points. The results showed that the protein levels of TRIM32 were gradually reduced along with the increased level of RTA expression (Fig. 4A), while no significant change at the transcription level of TRIM32 was observed (Fig. 4B). To further address if the regulation of RTA in the reduction of TRIM32 at protein levels is via proteasome degradation, we co-transfected myc-tagged TRIM32 or GFP-myc vector with different dosages of myc-tagged RTA into HEK293T cells,

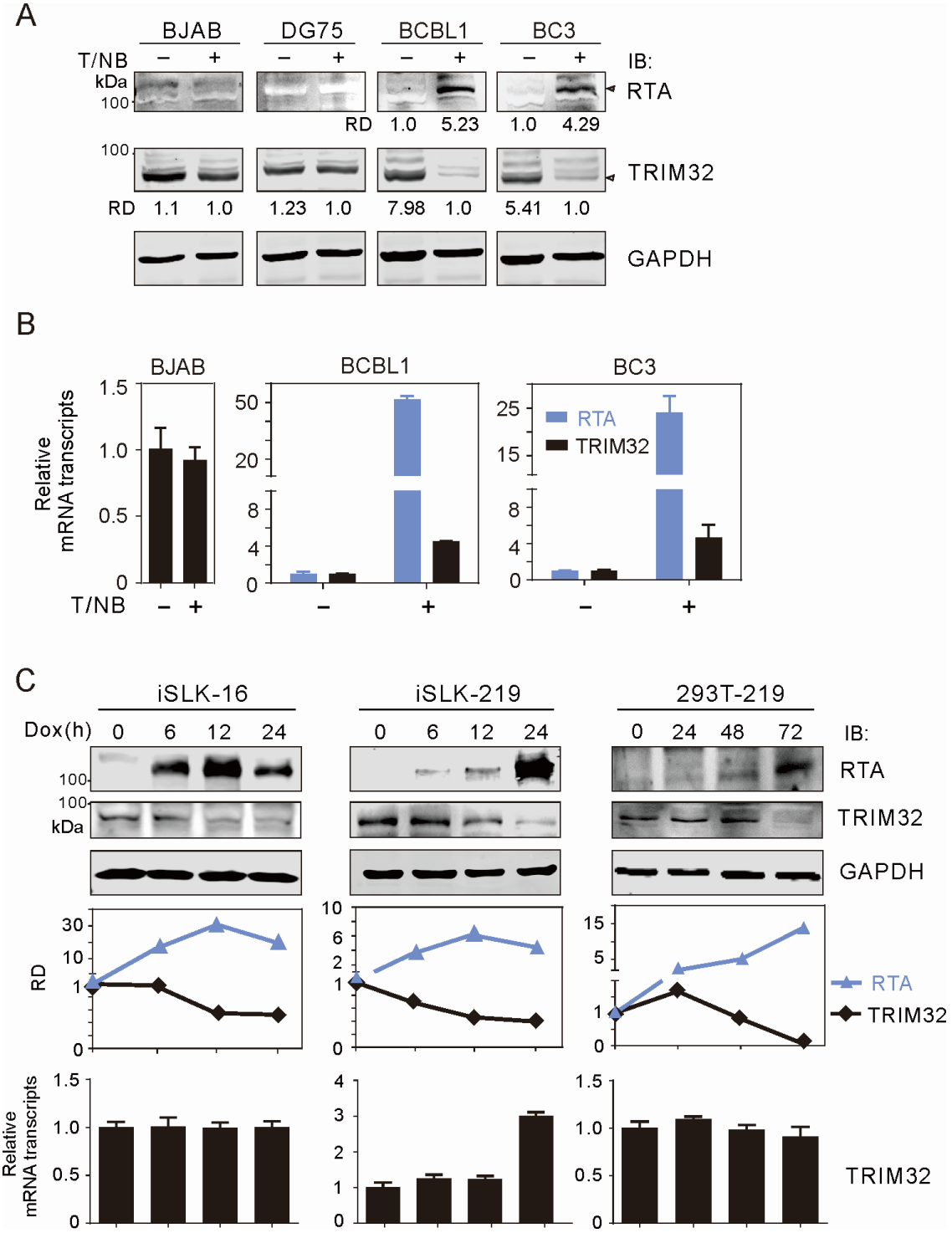

FIG 3 The protein level of TRIM32 is reduced in PEL cells with KSHV lytic reactivation. (A) Reactivation of KSHV in PEL cells dramatically reduced the protein level of TRIM32. Equal amounts of KSHV-infected PEL cells (BCBL1 and BC3) and uninfected B-lymphoma cells (BJAB and DG75) were individually treated with or without 20 ng/mL TPA (T) and 1.5 mM sodium butyrate (NB) for 20 h, followed by whole cell lysate for IB with antibodies as indicated. GAPDH was used as an internal control. RD of the protein level of TRIM32 or RTA was quantified and shown. (B) Reactivation of KSHV in PEL cells did not significantly impair the transcriptional level of TRIM32. Total RNA extracts from BCBL1, BC3, and BJAB cells treated with T/NB as in panel (A) were individually reversely transcribed and quantitative PCR analysis for TRIM32 transcripts. (C) Doxycycline-induced RTA expression in iSLK-16, iSLK-219, and 293T-219 cells led to the decreased protein level of TRIM32. Equal amounts of iSLK or 293T cells carrying doxycycline-induced RTA and KSHV whole genome were treated with Dox for different time points and subjected to IB with antibodies as indicated. RD of protein levels of RTA and TRIM32 was quantified and shown in the middle panels. The relative mRNA transcripts of TRIM32 were detected by quantitative PCR analysis and shown at the bottom panels.

followed by treatment with or without MG132 for the inhibition of proteasome activity. The results showed a significant reduction of TRIM32, but not GFP protein, observed along with the increase of RTA (Fig. 4C, upper panels), while the inhibition of proteasome activity by MG132 significantly blocked the degradation of TRIM32 (Fig. 4C, lower panels). Consistently, MG132 but not chloroquine (Chl) efficiently inhibited the RTA-induced degradation of TRIM32 in BCBL1 cells upon the reactivation of lytic replication (Fig. 4D). These data suggest that the degradation of TRIM32 induced by RTA is mainly dependent on the proteasome pathway, rather than the lysosomal pathway.

TRIM32 interacts with RTA through its transactivation domain

To determine whether TRIM32 physically interacts with RTA, HEK293T cells were co-transfected with GFP-tagged TRIM32 with or without myc-tagged RTA, followed by treatment with MG132 or dimethyl sulfoxide (DMSO). The co-immunoprecipitation (co-IP) results revealed an obvious interaction between RTA and TRIM32 (Fig. 5A). Interestingly, immunofluorescent assay data showed that when co-expressed with RTA, TRIM32 was translocated mainly in the nuclear compartment, and this translocation was further enhanced by the inhibition of proteasome activity (Fig. 5B). To further investigate if the interaction between RTA and TRIM32 exists in the KSHV-positive PEL cells during lytic reactivation, BCBL1 cells treated with TPA and sodium butyrate were subjected to co-immunoprecipitation with anti-RTA antibody followed by immunoblotting with TRIM32 antibody. Consistently, endogenous TRIM32 in BCBL1 cells showed physical interaction with RTA (Fig. 5C). MG132 treatment enhanced the accumulation and co-localization of TRIM32 with RTA at the nuclear compartment in BCBL1 cells upon reactivation of lytic replication (Fig. 5D), further confirmed by the interaction between RTA and TRIM32.

To identify which domain of TRIM32 is required for the interaction with RTA, four truncated mutants of TRIM32 with a GFP tag were generated by deleting different domains (Fig. 6A) and were individually co-expressed with or without RTA-myc in HEK293T cells. The whole cell lysate was subjected to co-immunoprecipitation with GFP antibody followed by immunoblotting against the myc-tag for RTA. To avoid the inhibitory effects of RTA on the degradation of TRIM32, the transfected cells were treated with MG132 before harvesting. As shown in Fig. 6A, the deletion of the NHL domain (ΔNHL) of TRIM32 significantly abolished the interaction of TRIM32 with RTA, when compared with full-length TRIM32 and other three truncated mutants [deletions of the RING domain (ΔRING), zinc finger domain (ΔB-box), or coiled-coil region (ΔCC)] separately. These results suggest that TRIM32 interacts with RTA through its substrate-binding NHL domain.

Since RTA can serve as an E3 ubiquitin ligase for several target substrates (47–49), to investigate whether the degradation of TRIM32 by RTA also relies on its E3 ligase activity, we generated various mutants of RTA within the RING finger domain (C131S, C141S, H145L, or ΔRING) and then individually co-expressed with exogenous GFP-tagged TRIM32 in 293T cells. Using wild-type RTA as a parallel control, immunoprecipitation assay results showed that site mutations within the RING domain of RTA significantly abrogated RTA-induced degradation of TRIM32 (Fig. 6B, right panel); in contrast, they did not alter the interaction between RTA and TRIM32 (Fig. 6B, left panel), suggesting that RTA can induce TRIM32 degradation through its E3 ligase activity.

RTA promotes K48-linked ubiquitylation of TRIM32

To determine whether RTA induces TRIM32 ubiquitylation via its E3 ligase activity, we performed experiments in ubiquitin-modified cells by co-expressing exogenous GFP-tagged TRIM32 with or without wild-type or RING-deleted RTA in the presence of HA-tagged ubiquitin in HEK293T cells. The results of co-IP assays with antibodies against GFP showed that a clear band of modified TRIM32 with ubiquitin was observed and only reduced in the presence of wild-type RTA, but not in the RING-deleted mutant (Fig. 7A, left panel). To further identify which lysine-linked form of ubiquitin participates in the modification of TRIM32 induced by RTA, we performed similar experiments with the

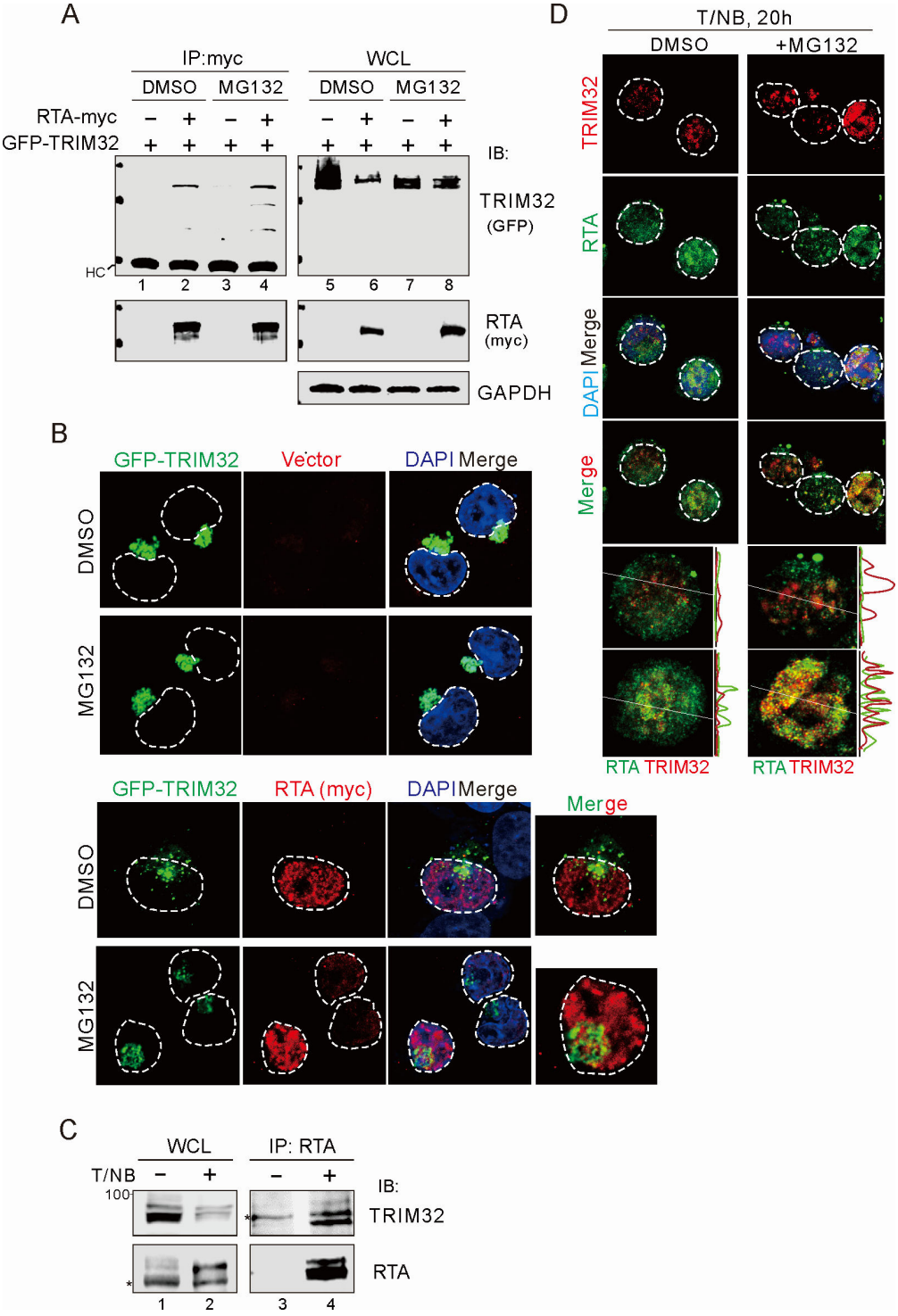

FIG 5 RTA physically interacts with TRIM32. (A) Ectopic expression of exogenous TRIM32 interacts with RTA. WCL from 293T cells co-transfected with different combinations of GFP-TRIM32 and RTA-myc in the presence of MG132 or DMSO treatment was subjected to IP followed by IB or direct immunoblotting assays as indicated in the figure. HC, heavy chain. (B) TRIM32 co-localizes with RTA at the nuclear compartment. HEK293T cells transfected with GFP-TRIM32 and RTA-myc in the presence of MG132 or DMSO were subjected to immunofluorescent confocal assays with antibodies against myc-tag (red) or GFP (green). The dashed white circle indicates the nuclear compartment. Nuclei were stained by 4′,6-diamidino-2-phenylindole (DAPI) (blue). (C) Endogenous TRIM32 associated with RTA in the KSHV-positive cells with lytic reactivation. WCLs from BCBL1 cells treated with 20 ng/mL of TPA and 1.5 mM sodium butyrate (T/NB) for 20 h were subjected to IP followed by IB or direct

(Continued on next page)

FIG 5 (Continued)

immunoblotting assays as indicated in the figure. The asterisk indicates a non-specific band. (D) Inhibitor of proteasome leads to accumulation and co-localization of TRIM32 with RTA at the nuclear compartment of PEL with KSHV reactivation. BCBL1 cells induced with 20 ng/mL of TPA and 1.5 mM sodium butyrate (T/NB) for 20 h, followed by treatment with or without MG132 for 8 h, were subjected to immunofluorescent assays with antibodies against TRIM32 and RTA. The dashed white circle indicates the nuclear compartment. Nuclei were stained by DAPI (blue). The enlarged merged view of TRIM32 and RTA is shown at the bottom panels.

ubiquitin mutant of only K6, K48, or K63 remained (all other lysines within ubiquitin were mutated). The results showed that with the exception of K48, neither K6- nor K63-linked ubiquitin modification of TRIM32 was reduced in the presence of wild-type RTA instead of its RING domain mutant (Fig. 7A, right panels). In agreement with this finding, the K48- not K63-linked form ubiquitinated endogenous TRIM32 was also dramatically increased in BCBL1 cells along with RTA expression upon reactivation of the lytic cycle (Fig. 7B, right panels). These data indicate that RTA promotes K48-linked ubiquitination of TRIM32.

Disruption of TRIM32 expression enhances the reactivation of KSHV lytic replication and virion production

To investigate the impact of TRIM32 on the cell survival and proliferation of KSHV-positive PEL cells, equal numbers of BCBL1 cells stable expressing shTRIM32 or shRNA were subjected to cell apoptosis analysis with flow cytometry at 72 h or inoculated and monitored for several days for cell proliferation and colony formation. Along with KSHV-negative B-lymphoma BJAB cells as a parallel control, the results showed that downregulating TRIM32 expression significantly induced cell apoptosis of BCBL1 cells, but not BJAB cells (Fig. 8A), suppressed cell proliferation (Fig. 8B), and led to much less colony formation (Fig. 8C), which suggest that the disruption of TRIM32 induces cell apoptosis of KSHV-positive PEL cells, but not KSHV-negative B-lymphoma cells.

To further address the effect of RTA-induced degradation of TRIM32 on PEL cell apoptosis upon KSHV reactivation, the protein levels of PARP-1 (a cell apoptotic marker) in BCBL1 cells stable expressing shTRIM32 or shRNA with or without TPA and sodium butyrate treatment were individually examined by immunoblotting assays. The results showed that the knockdown of TRIM32 induced more cleavage of PARP1 protein (Fig. 8D, compare lane 3 with 1) and more release of KSHV viral particles (Fig. 8E). Upon the reactivation of KSHV lytic replication, the protein levels of TRIM32 expression were significantly reduced and further hastened cellular apoptosis and augmented viral particle release, particularly in the TRIM32 knockdown group (Fig. 8D, compare lane 4 with 2; Fig. 8E). These findings suggest that KSHV reactivation could lead to TRIM32 degradation, thus enhancing cellular apoptosis and facilitating the production of virion particles upon reactivation.

DISCUSSION

Like other members of the herpesvirus family, the latent and lytic replication life cycle plays a critical role in KSHV-induced oncogenesis and pathogenesis (53), and a proportion of approximately 1%–3% of cells within KSHV tumor tissues undergo lytic activation (54). Upon stimulation or under certain conditions, KSHV will reactivate from the latent phase into the lytic replication phase, leading to a massive expression of the viral genes and the production of virion progeny (55, 56). Increasing evidence has shown that the activation of KSHV lytic gene expression plays a pivotal role in the onset and progression of several KSHV-associated cancers, including PEL, for regulating antiproliferative and antiapoptotic signaling pathways (57, 58). Previous studies from our group and colleagues have reported that the master regulator of lytic replication, RTA, not only inhibits the formation of the LANA-RBP-Jκ complex (50, 51) but also induces STAT6 for degradation via the proteasome and lysosome (52), during KSHV reactivation by stimuli of TPA and sodium butyrate. Although RTA has been previously shown to increase the

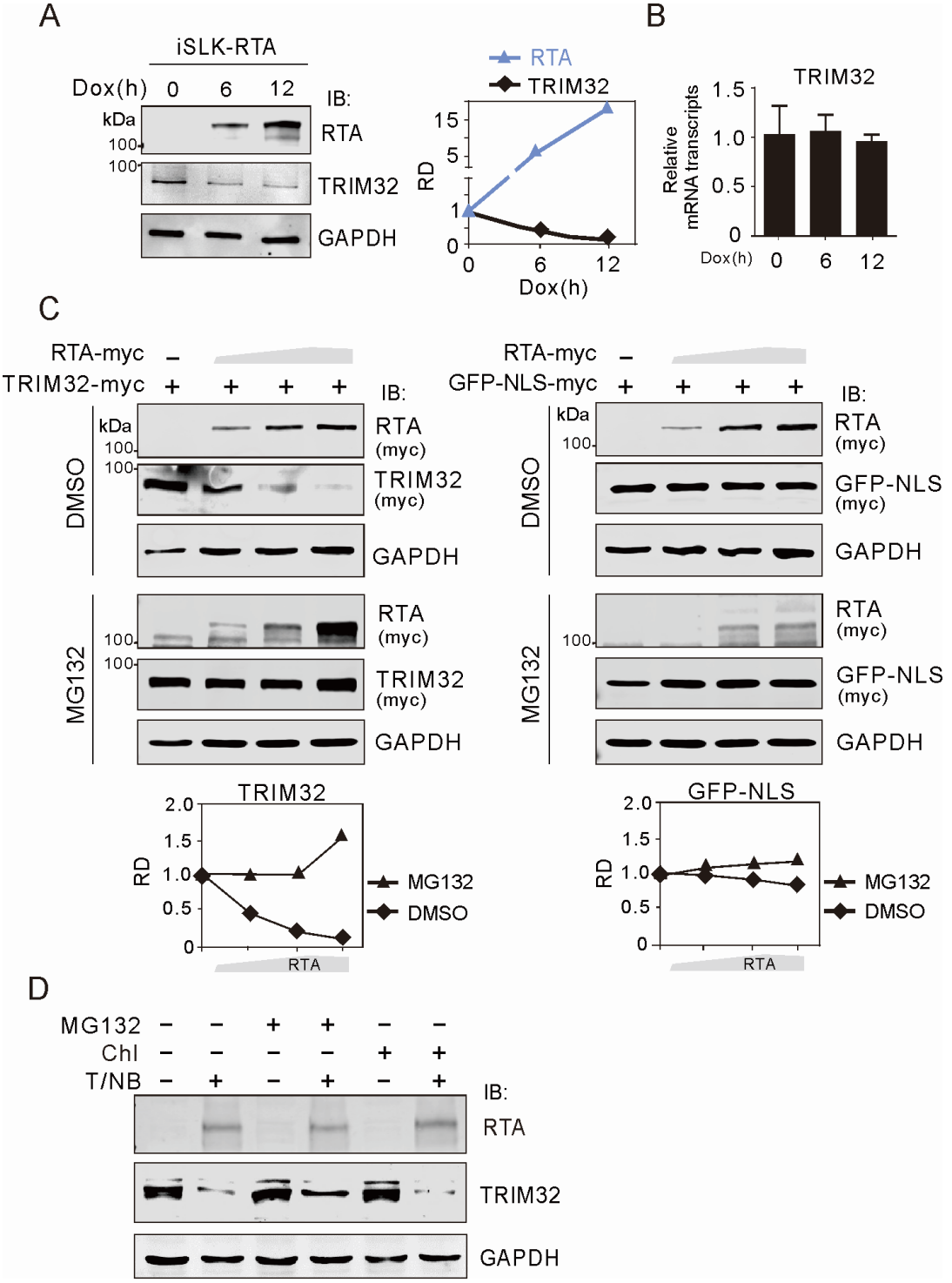

FIG 4 RTA-induced degradation of TRIM32 is dependent on the activity of proteasome not lysosome. (A) Doxycycline-induced RTA expression in iSLK-RTA cells reduced the protein level of TRIM32. iSLK cells carrying Dox-induced RTA (iSLK-RTA) were treated with doxycycline for different time points and subjected to IB with antibodies as indicated. RD of protein levels of RTA and TRIM32 was quantified and shown in the middle panel. (B) The relative mRNA transcripts of TRIM32 from panel (A) were detected by quantitative PCR analysis. (C) RTA induced TRIM32 degradation in a dose-dependent manner. HEK293T cells were co-transfected with 1 µg plasmid of TRIM32-myc or GFP-NLS-myc with different doses of RTA-myc (0, 0.5, 1, and 2 µg) and treated with MG132 for 8 h at 48 h post-transfection, followed by immunoblotting assays with antibodies as indicated. RD of TRIM32 and GFP protein bands was quantified and shown at the bottom panels. (D) Inhibitor of the proteasome, not lysosome, blocks RTA-induced degradation of TRIM32 during lytic reactivation. BCBL1 cells were induced with or without TPA and sodium butyrate (T/NB) for 12 h and then individually treated with MG132, Chl, or both for 12 h, followed by immunoblotting assays with antibodies as indicated in the figure.

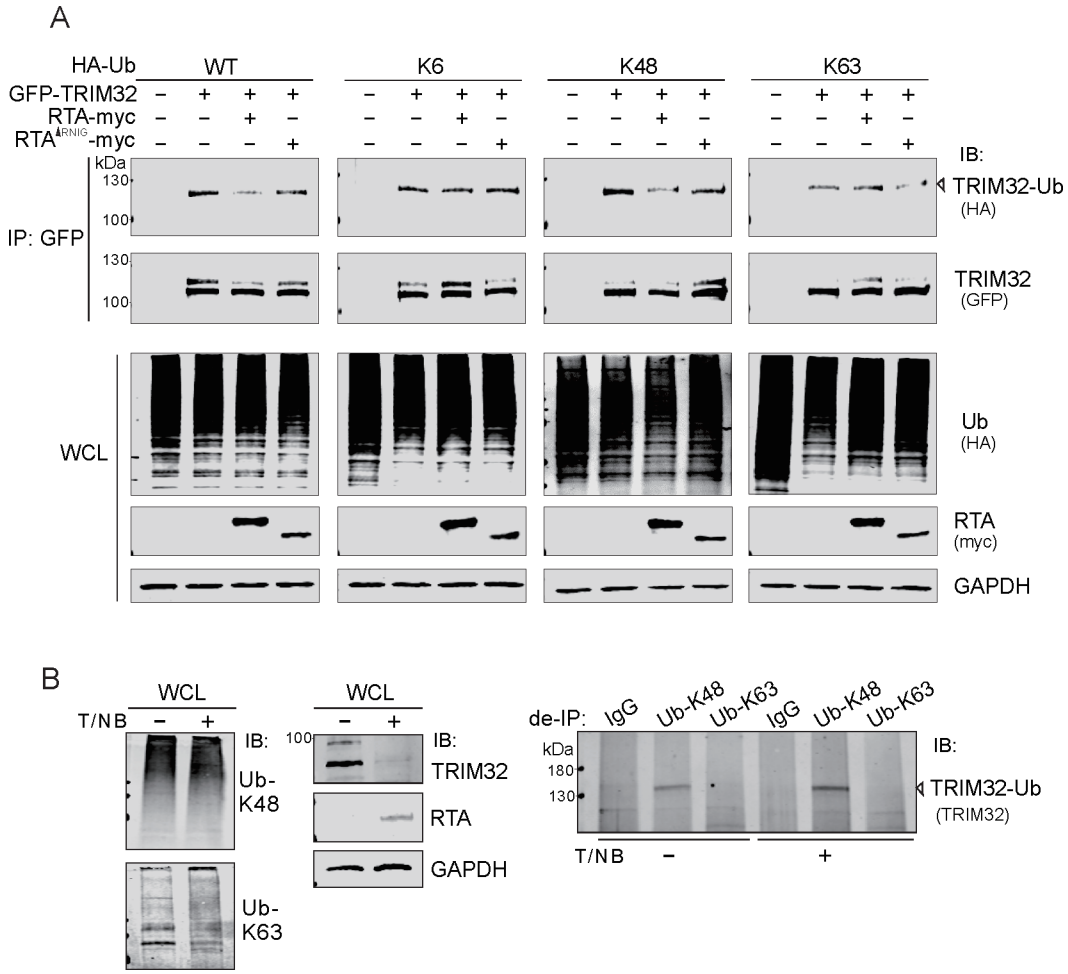

FIG 7 RTA promotes K48-linked ubiquitylation of TRIM32. (A) RTA induced K48-linked ubiquitylation of exogenous TRIM32. HEK293T cells were individually co-transfected with the indicated plasmids for 48 h. The WCLs were subjected to IP and IB assays as indicated. HA-tagged WT ubiquitin and its lysine mutants containing only K6, K48, or K63 were used. (B) K48-linked ubiquitylation of endogenous TRIM32 was significantly induced during KSHV reactivation. BCBL1 cells were exposed to TPA and sodium butyrate (T/NB) for 24 h, followed by treatment with MG132 for 8 h before cell harvest. WCLs were subjected to denatured immunoprecipitation (de-IP) using antibodies targeting K48 or K63 polyubiquitin, followed by IB as indicated in the figure.

expression and ubiquitylation of TRIML2 in the lytic phase (41), the role of RTA in other members of the TRIM family remains largely unknown. In this study, we revealed that TRIM32 was aberrantly expressed in KSHV latently infected cells, and the inhibition of TRIM32 is sufficient to activate RTA expression and lytic cycle. Moreover, the interaction between TRIM32 and RTA resulted in TRIM32 degradation via the proteasome pathway upon stimuli treatment for lytic reactivation, which in turn induces cell apoptosis and enhances viral progeny production (Fig. 8F), indicating that TRIM32 plays a critical role in controlling the KSHV life cycle.

Although several reports about the precise involvement of TRIM32 in the regulation of tumorigenesis remain controversial, our observations indicate that TRIM32 was aberrantly expressed in the KSHV latently infected cells, and the disruption of TRIM32 led to the activation of PARP1 cleavage and cell apoptosis and inhibition of PEL cell growth and colony formation, supporting the notion that TRIM32 functions as an oncoprotein. This agrees with previous reports that TRIM32 could function as ubiquitin E3 ligase for antiapoptosis and cell growth by targeting p53 and Abl2 for degradation (12–14). In addition, we observed that the inhibition of TRIM32 not only dramatically induces cell apoptosis in KSHV latently infected cells but also significantly enhances the expression of viral lytic protein RTA, indicating that TRIM32 may play critical dual roles in regulating

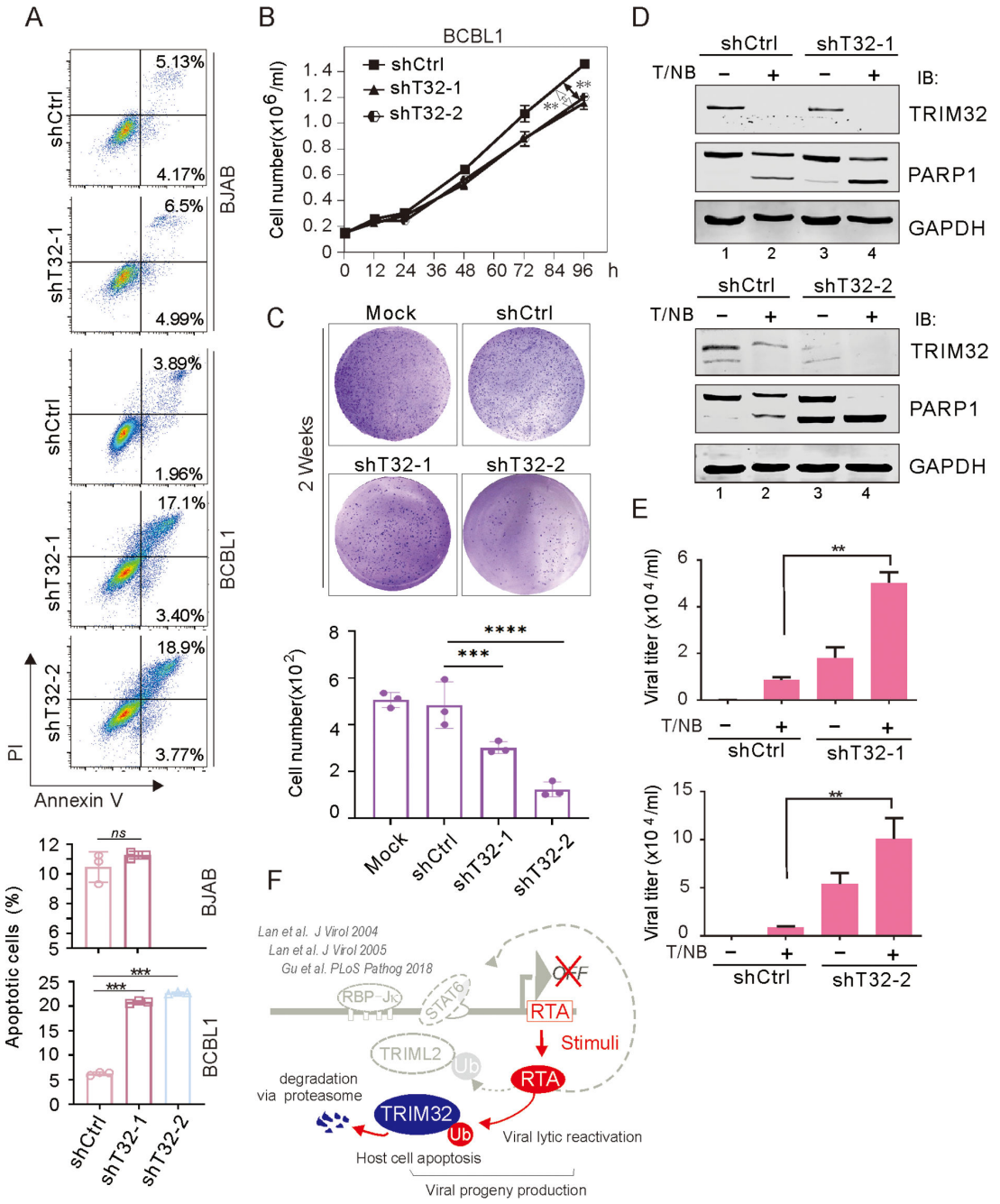

FIG 8 TRIM32 is required for KSHV to block viral lytic replication and drive cell proliferation. (A) The impact of TRIM32 knocked down on cell apoptosis. The KSHV-negative (BJAB) and -positive (BCBL1) cell lines were individually subjected to infection with lentivirus carrying shRNA against TRIM32 (shT32-1 or shT32-2) or luciferase control (shCtrl) for 72 h, followed by flow cytometry analysis for cell apoptosis. The percentage of cell apoptosis from three duplicated experiments was quantified and shown at the bottom panels. *ns*, no significant difference. Knockdown of TRIM32 reduces KSHV-infected (B) cell proliferation and (C) colony formation. Equal amounts of BCBL1 cells stable expressing shRNA against TRIM32 (shT32-1 or shT32-2) or luciferase control (shCtrl) were cultured and measured for cell proliferation at the specified time point by the cell vitality counter or inoculated for soft agar assays and then fixed on 14 days, followed by staining with crystal violet to determine the colony number (bottom panel). Data are presented as the mean ± SD of three independent experiments. Asterisks indicate significant differences ($^{**}P < 0.01$ and $^{***}P < 0.001$). (D) Knockdown of TRIM32 reduces the antiapoptosis ability of KSHV-infected PEL cells. BCBL1 cells with TRIM32 (shTRIM32-1 or shTRIM32-2) or luciferase control (shCtrl) stable knockdown were individually treated with or without TPA/NaB (T/NB) for 24 h and subjected to immunoblotting with antibodies as indicated in the figure. (E) TRIM32 knockdown enhances TPA- and sodium butyrate-induced KSHV virion production. The supernatants from equal amounts of cells in panel (D) were purified to quantify virion production. The statistical significance was evaluated, and $P < 0.05$ was indicated as double asterisks. (F) Proposed model of RTA-induced degradation of TRIM32 upon KSHV reactivation. During the reactivation of KSHV latently

(Continued on next page)

FIG 8 (Continued)

infected cells by stimuli (TPA and sodium butyrate), KSHV-encoded RTA has been previously reported to not only block the formation of LANA-RBP-Jκ complex (50, 51) but also induce STAT6 degradation via proteasome and lysosome (52). The results in this study further show that the interaction between TRIM32 and RTA leads to TRIM32 degradation via proteasome, which reduces cell proliferation and facilitates viral progeny production.

both host cellular and viral proteins. Furthermore, there are a couple of protein bands that appeared at the endogenous or exogenous expression of TRIM32, suggesting that the precise regulation of TRIM32 at the post-translational level is highly possible and may be dynamically targeted during the different stages of the viral life cycle. However, the related molecular mechanisms of TRIM32 regulation at the protein level during KSHV latent infection remain to be further investigated.

It has been demonstrated that RTA is the pivotal protein involved in regulating the transition of KSHV from latency to lytic replication (59), and subsequent investigations showed that RTA could act as a ubiquitin E3 ligase to selectively ubiquitylate different host cellular proteins, including STAT6 and TRIML2 for degradation or stabilization (41). Unlike the RTA-mediated STAT6 degradation via the proteasome and lysosome pathways, TRIM32 was targeted by proteasome instead of lysosome systems. Previous reports that TRIM32 is also shown to be involved in the regulation of autophagy (60) indicate that both TRIM32 and STAT6 may cooperate together or separately in controlling the herpes viral life cycle, which is required to be further investigated. In addition, previous reports showed that the NHL domain of TRIM32 is required for oligomerization and its autoubiquitination activity (10, 61). The fact that RTA interacts with TRIM32 through its NHL domain suggests that the NHL domain is the key target for the virus to regulate TRIM32 protein stability, and only the proteasome instead of the autophagy pathway is selectively targeted by KSHV for TRIM32 degradation during the lytic cycle, indicating that there are complex and important roles of TRIM32 in controlling KSHV latency and lytic replication.

Apoptosis is known as programmed cell death eliciting no inflammatory responses (62), which are regulated by multiple proteins including p53 and PARP1 (63). Although the inhibition of TRIM32 presents a similar effect as TRIML2 in previous observation to activate PARP1 cleavage for cell apoptosis, which is further enhanced upon stimuli of lytic reactivation (41), the influence on viral production upon reactivation is totally opposite, indicating that TRIM32 plays a different role from TRIML2 in regulating host cell apoptosis, which eventually facilitates the release of KSHV virus particles.

In summary, our finding revealed that the interaction between TRIM32 and RTA leads to the degradation of TRIM32 during viral lytic reactivation, which will contribute to the release of KSHV virion progeny production, highlighting the pivotal role of TRIM32 in governing the life cycle for herpesvirus pathogenesis, and may serve as a potential therapeutic target in KSHV-associated cancers.

MATERIALS AND METHODS

Cell culture and transfection

The KSHV-positive PEL (BC3, JSC1, BC1, and BCBL1) and KSHV-negative B-lymphoma (BJAB and DG75) cell lines from the American Type Culture Collection (ATCC) were maintained in a RPMI1640 medium supplemented with 10% fetal bovine serum (FBS) and 1% penicillin and streptomycin (Gibco-BRL). iSLK (1 µg/mL puromycin, 250 µg/mL G418) (64), iSLK-RTA (250 µg/mL G418, 100 µg/mL hygromycin) (65), iSLK-Bac16 (K-iSLK, 1.1 mg/mL hygromycin, 250 µg/mL G418, and 1 µg/mL puromycin) (64), iSLK-219 (1.1 mg/mL hygromycin, 250 µg/mL G418, and 4 µg/mL puromycin) (65), and rat endothelial MM and KMM (150 µg/mL hygromycin) cells (66) were kindly provided by Shou-Jiang Gao at the University of South California and were maintained in Dulbecco's modified Eagle's medium (DMEM) supplemented with 10% fetal bovine serum (FBS) and 1% penicillin and streptomycin (Gibco-BRL) (41). HEK293T (ATCC) cells were maintained in a

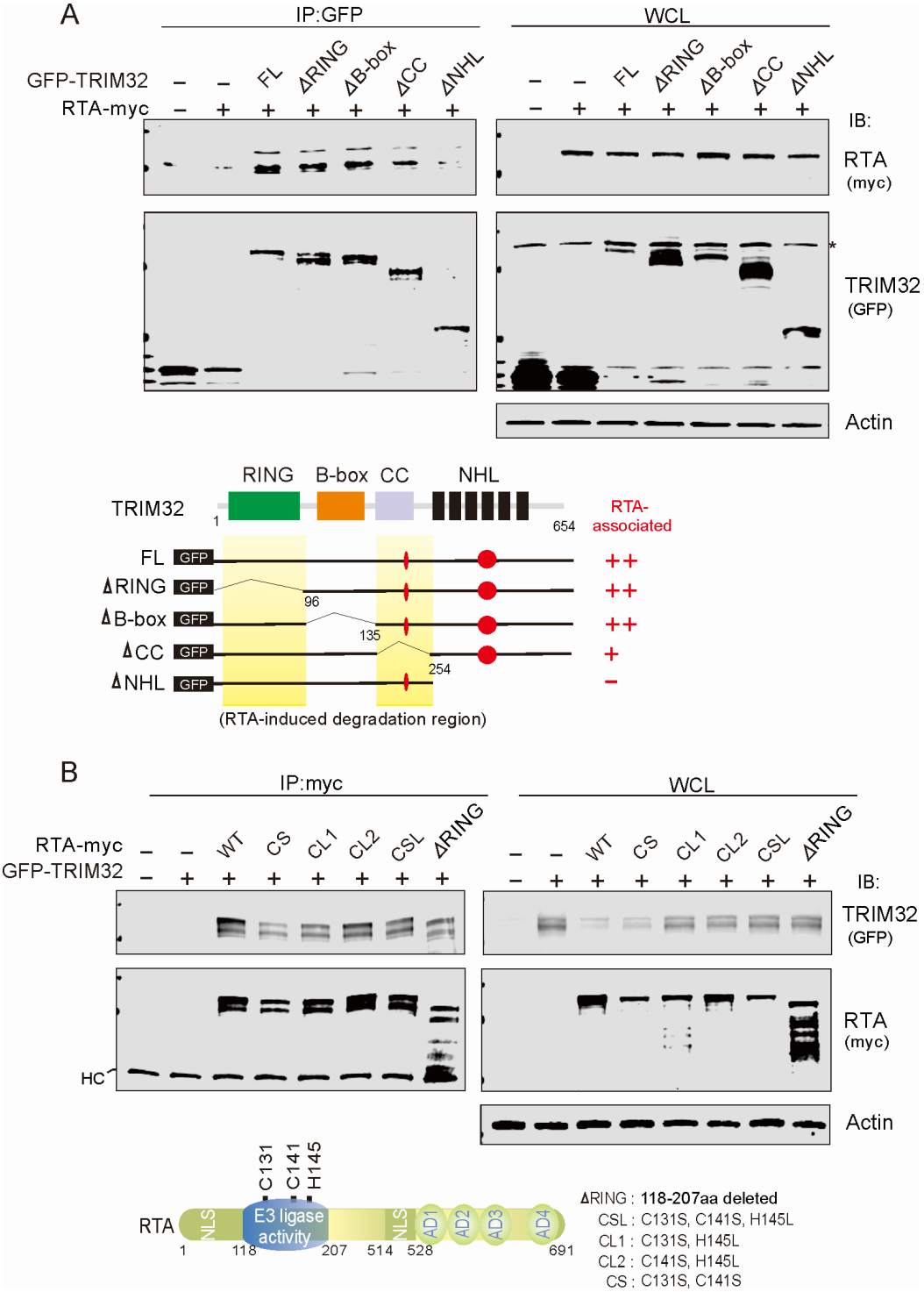

FIG 6 RTA-induced degradation of TRIM32 relies on the RING domain of RTA. (A) RTA associated with the NHL domain of TRIM32. HEK293T cells were transfected with the indicated plasmids for 48 h, and the WCLs were subjected to IP followed by IB or direct immunoblotting assays with the indicated antibodies. Schematic of the TRIM32 amino acid sequence and its truncation mutants was shown at the bottom panels. The red circle indicates the RTA-associated domains. The domains of RING, B-box, coil-coil (CC), and NHL are shown. (B) RTA-induced degradation of TRIM32 was dependent on its RING domain. HEK293T were transfected with TRIM32 with GFP tag in the presence or absence of wild-type (WT) RTA with myc-tag or its mutants for 48 h and subjected to IB with antibodies as indicated in the figure. A brief schematic of the RTA amino acid sequence and its mutants is shown at the bottom panels.

DMEM medium supplemented with 10% FBS and 1% penicillin and streptomycin (Gibco-BRL). All cell lines were incubated at 37°C in a humidified environmental incubator with 5% CO_2. Cells were cultured 24 h before transfection with cell confluence reaching 60%–70%. HEK293T cells were transfected with 1 mg/mL polyethylenimine Linear (PEI) MW40000 (40816ES03, Yeasen) at a ratio of 1 µg plasmid DNA:3 µL PEI and incubated for 48 h.

Reagents and antibodies

Mouse antibodies to GFP (50430-2-AP), myc-tag (60003-2-Ig), and GAPDH (60004-1-Ig) were purchased from Proteintech Group (Wuhan, China). Alexa Fluor 488-conjugated goat anti-rabbit IgG (H+L) (cat# 2072687, Invitrogen), Alexa Fluor 488-conjugated goat anti-mouse IgG (H+L) (cat# 1942237, Invitrogen), Alexa Fluor 594-conjugated goat anti-rabbit IgG (H+L) (cat# 111-585-003, Invitrogen), and Alexa Fluor 594-conjugated goat anti-mouse IgG (H+L) (cat# A-11032, Invitrogen) antibodies were purchased from Invitrogen Co. Ltd. Mouse monoclonal antibodies against RTA (4D2, a gift from Ke Lan at Wuhan University), myc (9E10, stored in the lab), and LANA (LANA1, stored in the lab) were individually prepared from hybridoma cultures. Rabbit antibodies against Flag polyAb (F1804; Sigma-Aldrich) or TRIM32 (ab96612, Abcam) and mouse antibodies against PARP1 (F2, Santa Cruz) were used in this study. The DAPI (cat# C006, Solarbio) and sodium butyrate (S615175, J&K Corporation) were used in chemical treatment assays. Proteasome inhibitor MG132 was purchased from Biomol International, and TPA and Chl were purchased from Sigma-Aldrich. Dox was purchased from Sangon Biotech (Shanghai). Protease inhibitors of phenylmethanesulfonyl fluoride (PMSF), leupeptin, aprotinin, pepstatin A, and puromycin were purchased from Amresco, and G418 from Inalco S.p.A.

DNA constructs

Plasmid TRIM32-myc was obtained by PCR amplicon (with cDNA from BJAB genome as template) and subcloned into pcDNA3.1-3xmyc vector at *Eco*R*I and Hin*dIII sites. Plasmid TRIM32-FLAG was obtained by PCR amplicon (with TRIM32-myc as template) and subcloned into pcDNA3.1-FLAG vector at *No*t1 and *Hin*dIII sites. The wild type of TRIM32 with a GFP tag at the amino terminus and its deleted mutants (ΔRING, ΔB-box, ΔCC, or ΔNHL) were generated by PCR amplicon (with TRIM32-FLAG as template) and subcloned into pEGFP-C1 vector at *Kpn*I and *Bam*HI sites. The RING domain deleted mutant (ΔRING) was constructed by deleting the DNA fragment of 1–288 nt in the ORF of TRIM32. The B-box domain deleted mutant (ΔB-box) was constructed by deleting the DNA fragment of 288–405 nt in the ORF of TRIM32. The coiled-coil domain deleted mutant (ΔCC) was constructed by deleting the DNA fragment of 405–762 nt in the ORF of TRIM32. The NHL domain deleted mutant (ΔNHL) was constructed by deleting the DNA fragment of 762–1,962 nt in the ORF of TRIM32. Plasmids RTA-myc and its mutants (ΔRING), CS (C131S, C141S), CL1 (C131S, H145L), CL2 (C141S, H145L), and CSL (C131S, C141S, and H145L), RFP-RTA, and pCDNA3.1-GFP-NLS-myc were described as previously (41).

Immunofluorescence assays

HEK293T cells were transfected with plasmids as indicated. After transfection for 24 h, these cells were then fixed with 4% paraformaldehyde (PFA) and permeabilized in phosphate-buffered saline (PBS) containing 0.2% fish skin gelatin (G-7765; Sigma) and 0.2% Triton X-100 for 30 min, respectively. For BCBL1 cells, the cells after treatment were fixed with 4% PFA and gently spread on the coverslip and dried in a 37°C oven for 10 min, with the following operations as described above. Finally, cells were incubated with the indicated primary and secondary antibodies and nuclear staining with DAPI, then visualized with a Leica SP8 confocal microscope.

Generation of knockdown cell lines

A pGIPz vector plasmid containing shRNA-1 (5′-GAAGTTGAGAAGTCCAATA-3′) and shRNA-2 (5′-GGTGGAAAGCTTTGGTGTT-3′) targeting the TRIM32 gene was constructed and transduced into BJAB or BCBL1 cells. Transduction was followed by selection via culture with 1 µg/mL puromycin for 1 week. Surviving cells were cultured in a 10% FBS medium. Knockdown efficiency was then verified by reverse transcription quantitative PCR or immunoblotting.

Immunoprecipitation and immunoblotting

IP and IB assays were performed as described previously (41). For IP, cell samples were collected at the indicated times and lysed on ice for 30 min using NP-40 lysis buffer (20 mM Tris-HCl, 150 mM NaCl, 1% NP-40, and 1 mM EDTA) with protease inhibitors, followed by centrifugation to collect the supernatant (14,500 rpm, 10 min) and incubation of the supernatant with the corresponding primary antibody at 4°C overnight. A protein of interest complex was captured with protein A/G sepharose beads and boiled in a loading buffer. For denature IP, cell samples were collected at the indicated times and denatured using NP-40 denatured buffer (20 mM Tris-HCl, 150 mM NaCl, 1% NP-40, 1 mM EDTA, and 2% SDS) with protease inhibitors, subsequently boiled for 10 min, and then lysed on ice using NP-40 lysis buffer, followed by the regular IP as described above. For IB, the cell lysates and immunoprecipitants were resolved by the appropriate concentration of sodium dodecyl sulfate polyacrylamide gel electrophoresis and then transferred to the nitrocellulose membrane. After incubation with the indicated primary and secondary antibodies, the membranes were scanned with an Odyssey Infrared scanner (Li-Cor Biosciences). Densitometric analysis was performed with the Odyssey scanning software.

Cell proliferation assay

BCBL1 cells stable carrying TRIM32 shRNA or luciferase control shRNA (shCTRL) were plated in a T25 flask and incubated for 24 h. After different culture time points, the cells were collected and counted using a Vi-Cell XR (Beckman Coulter) at different time points. The culture medium is replaced every 24 h.

Colony formation assay

The soft agar colony formation assay was performed as described previously (67). Briefly, a bottom layer containing 0.75% agar in 10% FBS RPMI1640 was prepared first, followed by an appropriate number of cells in a 0.36 mixture for the top layer. The dish with two layers was incubated at 37°C for 3 weeks, and then, the colonies were stained with a solution of 0.04% crystal–2% ethanol in PBS and counted using count PHICS software for ImageJ (68).

Quantitative real-time PCR

Total RNA was extracted from cells by using TRIzol and reverse-transcribed to cDNA using a kit from TransScript First-Strand cDNA Synthesis SuperMix (Beijing TransGen Biotech Co., Ltd) according to the manufacturer's protocol. The cDNA was amplified in a 20 µL total volume with 10 µL SYBR Green, 0.4 µL each primer (10 µM), 4.2 µL H_2O, and 5 µL cDNA. A melting-curve analysis confirmed the specificity of the amplified products. Relative levels of change were calculated using the threshold cycle (ΔΔCT) method, and samples were tested in triplicates. GAPDH was used as an internal control.

Purification and quantitation of KSHV virion

The BCBL1 cells with or without TRIM32 knockdown cells were treated with 20 ng/mL of TPA and 1.5 mM sodium butyrate (J&K Corporation) for 2 days at 37°C with 5% CO_2. After treatment, the supernatant of the culture medium was collected and filtered through

a 0.45 µm filter, and viral particles were spun down at 25,000 rpm for 2 h at 4°C. The concentrated virus was collected and used for virion quantitation by quantitative PCR as described previously (41).

Cell apoptosis analysis

The apoptotic cells were analyzed by using an Annexin V-FITC/PI apoptosis detection kit (Yeasen, #40302ES50) according to the manufacturer's instructions. Briefly, cells were harvested and washed twice with PBS and suspended in the binding buffer. The cells were then incubated with Annexin V-FITC and PI in the dark for 10 min at room temperature and subjected to flow cytometric analysis by using a BD FACSCalibur flow cytometer (BD Biosciences) and analyzed with FlowJo software.

Statistical analysis

Statistical significance of difference was used for unpaired two-tailed Student's *t*-test with GraphPad Prism software. Each experiment was performed at least three times (unless specified otherwise) and calculated for the mean and standard deviation.

ACKNOWLEDGMENTS

We are grateful to Shou-Jiang Gao from the University of Pittsburgh and Ke Lan from Wuhan University for providing reagents. We thank members of the Cai laboratory for their technical assistance and helpful discussions and the staff from the core facility of microbiology and parasitology of SHMC for the technical support.

This work was supported by the National Natural Science Foundation of China (32120103001, 82272324, 82102386, and 82372242), National Key Research and Development Program of China (2023YFC2306702 and 2021YFA1300803), Program of Shanghai Academic Research Leader (22XD1403000), Shanghai Municipal Science and Technology Project (23JC1401302 and ZD2021CY001), and Jinan University and Institute Innovation Program (2020GXRC043). Q.C. is a scholar of the New Century Excellent Talents at the University of China and Oriental Talent Leader of Shanghai.

Q.C., F.W., Y.W., and Y.Z. conceived the project and designed the experiments. Y.Z., Z.D., F.G., Y.X., Y.L., W.S., W.R., S.D., and C.Z. performed the experiments. Q.C., F.W., W.Y., Y.Z., Z.D., F.G., Y.X., and Y.L. analyzed the data. Y.Z. and Y.W. wrote the manuscript. F.W. and Q.C. revised the manuscript.

AUTHOR AFFILIATIONS

[1]MOE/NHC/CAMS Key Laboratory of Medical Molecular Virology, Shanghai Institute of Infections Disease and Biosecurity, Shanghai Frontiers Science Center of Pathogenic Microorganism and Infection, School of Basic Medical Science, Shanghai Medical College, Fudan University, Shanghai, China
[2]ShengYushou Center of Cell Biology and Immunology, Joint International Research Laboratory of Metabolic & Development Sciences, School of Life Sciences and Biotechnology, Shanghai Jiao Tong University, Shanghai, China

AUTHOR ORCIDs

Yuyan Wang http://orcid.org/0000-0002-1326-6831
Fang Wei http://orcid.org/0000-0001-8964-1645
Qiliang Cai http://orcid.org/0000-0002-7147-0953

FUNDING

Funder	Grant(s)	Author(s)
MOST | National Natural Science Foundation of China (NSFC)	32120103001	Qiliang Cai
MOST | National Key Research and Development Program of China	2023YFC2306702, 2021YFA1300803	Qiliang Cai

DATA AVAILABILITY

All data from this study are included within this article and are available from the lead contact (Qiliang Cai, qiliang@fudan.edu.cn) upon request.

REFERENCES

1. Hatakeyama S. 2017. TRIM family proteins: roles in autophagy, immunity, and carcinogenesis. Trends Biochem Sci 42:297–311. https://doi.org/10.1016/j.tibs.2017.01.002
2. Torok M, Etkin LD. 2001. Two B or not two B? Overview of the rapidly expanding B-box family of proteins. Differentiation 67:63–71. https://doi.org/10.1046/j.1432-0436.2001.067003063.x
3. Massiah MA, Simmons BN, Short KM, Cox TC. 2006. Solution structure of the RBCC/TRIM B-box1 domain of human MID1: B-box with a RING. J Mol Biol 358:532–545. https://doi.org/10.1016/j.jmb.2006.02.009
4. Li X, Li Y, Stremlau M, Yuan W, Song B, Perron M, Sodroski J. 2006. Functional replacement of the RING, B-box 2, and coiled-coil domains of tripartite motif 5alpha (TRIM5alpha) by heterologous TRIM domains. J Virol 80:6198–6206. https://doi.org/10.1128/JVI.00283-06
5. Xie C, Powell C, Yao M, Wu J, Dong Q. 2014. Ubiquitin-conjugating enzyme E2C: a potential cancer biomarker. Int J Biochem Cell Biol 47:113–117. https://doi.org/10.1016/j.biocel.2013.11.023
6. Waterman H, Levkowitz G, Alroy I, Yarden Y. 1999. The RING finger of c-Cbl mediates desensitization of the epidermal growth factor receptor. J Biol Chem 274:22151–22154. https://doi.org/10.1074/jbc.274.32.22151
7. Bell JL, Malyukova A, Holien JK, Koach J, Parker MW, Kavallaris M, Marshall GM, Cheung BB. 2012. TRIM16 acts as an E3 ubiquitin ligase and can heterodimerize with other TRIM family members. PLoS One 7:e37470. https://doi.org/10.1371/journal.pone.0037470
8. Short KM, Cox TC. 2006. Subclassification of the RBCC/TRIM superfamily reveals a novel motif necessary for microtubule binding. J Biol Chem 281:8970–8980. https://doi.org/10.1074/jbc.M512755200
9. Lazzari E, Meroni G. 2016. TRIM32 ubiquitin E3 ligase, one enzyme for several pathologies: from muscular dystrophy to tumours. Int J Biochem Cell Biol 79:469–477. https://doi.org/10.1016/j.biocel.2016.07.023
10. Tocchini C, Ciosk R. 2015. TRIM-NHL proteins in development and disease. Semin Cell Dev Biol 47–48:52–59. https://doi.org/10.1016/j.semcdb.2015.10.017
11. Bawa S, Piccirillo R, Geisbrecht ER. 2021. TRIM32: a multifunctional protein involved in muscle homeostasis, glucose metabolism, and tumorigenesis. Biomolecules 11:408. https://doi.org/10.3390/biom11030408
12. Horn EJ, Albor A, Liu Y, El-Hizawi S, Vanderbeek GE, Babcock M, Bowden GT, Hennings H, Lozano G, Weinberg WC, Kulesz-Martin M. 2004. RING protein TRIM32 associated with skin carcinogenesis has anti-apoptotic and E3-ubiquitin ligase properties. Carcinogenesis 25:157–167. https://doi.org/10.1093/carcin/bgh003
13. Kano S, Miyajima N, Fukuda S, Hatakeyama S. 2008. Tripartite motif protein 32 facilitates cell growth and migration via degradation of Abl-interactor 2. Cancer Research 68:5572–5580. https://doi.org/10.1158/0008-5472.CAN-07-6231
14. Liu J, Zhang C, Wang XL, Ly P, Belyi V, Xu-Monette ZY, Young KH, Hu W, Feng Z. 2014. E3 ubiquitin ligase TRIM32 negatively regulates tumor suppressor p53 to promote tumorigenesis. Cell Death Differ 21:1792–1804. https://doi.org/10.1038/cdd.2014.121
15. McManus DC, Lefebvre CA, Cherton-Horvat G, St-Jean M, Kandimalla ER, Agrawal S, Morris SJ, Durkin JP, Lacasse EC. 2004. Loss of XIAP protein expression by RNAi and antisense approaches sensitizes cancer cells to functionally diverse chemotherapeutics. Oncogene 23:8105–8117. https://doi.org/10.1038/sj.onc.1207967
16. Ryu YS, Lee Y, Lee KW, Hwang CY, Maeng JS, Kim JH, Seo YS, You KH, Song B, Kwon KS. 2011. TRIM32 protein sensitizes cells to tumor necrosis factor (TNFα)-induced apoptosis via its RING domain-dependent E3 ligase activity against X-linked inhibitor of apoptosis (XIAP). J Biol Chem 286:25729–25738. https://doi.org/10.1074/jbc.M111.241893
17. Tong QS, Zheng LD, Wang L, Zeng FQ, Chen FM, Dong JH, Lu GC. 2005. Downregulation of XIAP expression induces apoptosis and enhances chemotherapeutic sensitivity in human gastric cancer cells. Cancer Gene Ther 12:509–514. https://doi.org/10.1038/sj.cgt.7700813
18. Uchil PD, Hinz A, Siegel S, Coenen-Stass A, Pertel T, Luban J, Mothes W. 2013. TRIM protein-mediated regulation of inflammatory and innate immune signaling and its association with antiretroviral activity. J Virol 87:257–272. https://doi.org/10.1128/JVI.01804-12
19. Khan R, Khan A, Ali A, Idrees M. 2019. The interplay between viruses and TRIM family proteins. Rev Med Virol 29:e2028. https://doi.org/10.1002/rmv.2028
20. Ozato K, Shin DM, Chang TH, Morse HC. 2008. TRIM family proteins and their emerging roles in innate immunity. Nat Rev Immunol 8:849–860. https://doi.org/10.1038/nri2413
21. Heaton SM, Borg NA, Dixit VM. 2016. Ubiquitin in the activation and attenuation of innate antiviral immunity. J Exp Med 213:1–13. https://doi.org/10.1084/jem.20151531
22. Zhang J, Hu MM, Wang YY, Shu HB. 2012. TRIM32 protein modulates type I interferon induction and cellular antiviral response by targeting MITA/STING protein for K63-linked ubiquitination. J Biol Chem 287:28646–28655. https://doi.org/10.1074/jbc.M112.362608
23. Yang Q, Liu TT, Lin H, Zhang M, Wei J, Luo WW, Hu YH, Zhong B, Hu MM, Shu HB. 2017. TRIM32-TAX1BP1-dependent selective autophagic degradation of TRIF negatively regulates TLR3/4-mediated innate immune responses. PLoS Pathog 13:e1006600. https://doi.org/10.1371/journal.ppat.1006600
24. Gessain A, Sudaka A, Brière J, Fouchard N, Nicola MA, Rio B, Arborio M, Troussard X, Audouin J, Diebold J, de Thé G. 1996. Kaposi sarcoma-associated herpes-like virus (human herpesvirus type 8) DNA sequences in multicentric Castleman's disease: is there any relevant association in non-human immunodeficiency virus-infected patients? Blood 87:414–416.
25. Chang Y, Moore PS. 1996. Kaposi's sarcoma (KS)-associated herpesvirus and its role in KS. Infect Agents Dis 5:215–222.
26. Longnecker R, Neipel F. 2007. Introduction to the human γ-herpesviruses. In Arvin A, Campadelli-Fiume G, Mocarski E, Moore PS, Roizman B, Whitley R, Yamanishi K (ed), Human herpesviruses: biology, therapy, and immunoprophylaxis. Cambridge University, Cambridge.
27. Mesri EA, Cesarman E, Boshoff C. 2010. Kaposi's sarcoma and its associated herpesvirus. Nat Rev Cancer 10:707–719. https://doi.org/10.1038/nrc2888
28. Pan H, Zhou F, Gao SJ. 2004. Kaposi's sarcoma-associated herpesvirus induction of chromosome instability in primary human endothelial cells. Cancer Res 64:4064–4068. https://doi.org/10.1158/0008-5472.CAN-04-0657

29. Sadagopan S, Sharma-Walia N, Veettil MV, Raghu H, Sivakumar R, Bottero V, Chandran B. 2007. Kaposi's sarcoma-associated herpesvirus induces sustained NF-kappaB activation during de novo infection of primary human dermal microvascular endothelial cells that is essential for viral gene expression. J Virol 81:3949–3968. https://doi.org/10.1128/JVI.02333-06
30. Ye FC, Blackbourn DJ, Mengel M, Xie JP, Qian LW, Greene W, Yeh IT, Graham D, Gao SJ. 2007. Kaposi's sarcoma-associated herpesvirus promotes angiogenesis by inducing angiopoietin-2 expression via AP-1 and Ets1. J Virol 81:3980–3991. https://doi.org/10.1128/JVI.02089-06
31. Dourmishev LA, Dourmishev AL, Palmeri D, Schwartz RA, Lukac DM. 2003. Molecular genetics of Kaposi's sarcoma-associated herpesvirus (human herpesvirus-8) epidemiology and pathogenesis. Microbiol Mol Biol Rev 67:175–212. https://doi.org/10.1128/MMBR.67.2.175-212.2003
32. Jenner RG, Albà MM, Boshoff C, Kellam P. 2001. Kaposi's sarcoma-associated herpesvirus latent and lytic gene expression as revealed by DNA arrays. J Virol 75:891–902. https://doi.org/10.1128/JVI.75.2.891-902.2001
33. Gradoville L, Gerlach J, Grogan E, Shedd D, Nikiforow S, Metroka C, Miller G. 2000. Kaposi's sarcoma-associated herpesvirus open reading frame 50/Rta protein activates the entire viral lytic cycle in the HH-B2 primary effusion lymphoma cell line. J Virol 74:6207–6212. https://doi.org/10.1128/jvi.74.13.6207-6212.2000
34. Sun R, Lin SF, Gradoville L, Yuan Y, Zhu F, Miller G. 1998. A viral gene that activates lytic cycle expression of Kaposi's sarcoma-associated herpesvirus. Proc Natl Acad Sci U S A 95:10866–10871. https://doi.org/10.1073/pnas.95.18.10866
35. Strahan RC, McDowell-Sargent M, Uppal T, Purushothaman P, Verma SC. 2017. KSHV encoded ORF59 modulates histone arginine methylation of the viral genome to promote viral reactivation. PLoS Pathog 13:e1006482. https://doi.org/10.1371/journal.ppat.1006482
36. Rossetto C, Gao Y, Yamboliev I, Papousková I, Pari G. 2007. Transcriptional repression of K-Rta by Kaposi's sarcoma-associated herpesvirus K-bZIP is not required for oriLyt-dependent DNA replication. Virology 369:340–350. https://doi.org/10.1016/j.virol.2007.08.019
37. Verma D, Li DJ, Krueger B, Renne R, Swaminathan S. 2015. Identification of the physiological gene targets of the essential lytic replicative Kaposi's sarcoma-associated herpesvirus ORF57 protein. J Virol 89:1688–1702. https://doi.org/10.1128/JVI.02663-14
38. Wang SE, Wu FY, Yu Y, Hayward GS. 2003. CCAAT/enhancer-binding protein-alpha is induced during the early stages of Kaposi's sarcoma-associated herpesvirus (KSHV) lytic cycle reactivation and together with the KSHV replication and transcription activator (RTA) cooperatively stimulates the viral RTA, MTA, and PAN promoter. J Virol 77:9590–9612. https://doi.org/10.1128/jvi.77.17.9590-9612.2003
39. Katano H, Sato Y, Itoh H, Sata T. 2001. Expression of human herpesvirus 8 (HHV-8)-encoded immediate early protein, open reading frame 50, in HHV-8-associated diseases. J Hum Virol 4:96–102.
40. Zhao Q, Liang D, Sun R, Jia B, Xia T, Xiao H, Lan K. 2015. Kaposi's sarcoma-associated herpesvirus-encoded replication and transcription activator impairs innate immunity via ubiquitin-mediated degradation of myeloid differentiation factor 88. J Virol 89:415–427. https://doi.org/10.1128/JVI.02591-14
41. Gu F, Wang C, Wei F, Wang Y, Zhu Q, Ding L, Xu W, Zhu C, Cai C, Qian Z, Yuan Z, Robertson E, Cai Q. 2018. STAT6 degradation and ubiquitylated TRIML2 are essential for activation of human oncogenic herpesvirus. PLoS Pathog 14:e1007416. https://doi.org/10.1371/journal.ppat.1007416
42. Cui H, Liu Y, Huang Y. 2017. Roles of TRIM32 in corneal epithelial cells after infection with herpes simplex virus. Cell Physiol Biochem 43:801–811. https://doi.org/10.1159/000481563
43. Bodda C, Reinert LS, Fruhwürth S, Richardo T, Sun C, Zhang B-C, Kalamvoki M, Pohlmann A, Mogensen TH, Bergström P, Agholme L, O'Hare P, Sodeik B, Gyrd-Hansen M, Zetterberg H, Paludan SR. 2020. HSV1 VP1-2 deubiquitinates STING to block type I interferon expression and promote brain infection. J Exp Med 217:e20191422. https://doi.org/10.1084/jem.20191422
44. Ballestas ME, Kaye KM. 2001. Kaposi's sarcoma-associated herpesvirus latency-associated nuclear antigen 1 mediates episome persistence through cis-acting terminal repeat (TR) sequence and specifically binds TR DNA. J Virol 75:3250–3258. https://doi.org/10.1128/JVI.75.7.3250-3258.2001
45. Uppal T, Banerjee S, Sun Z, Verma SC, Robertson ES. 2014. KSHV LANA--the master regulator of KSHV latency. Viruses 6:4961–4998. https://doi.org/10.3390/v6124961
46. Spires LM, Wind E, Papp B, Toth Z. 2023. KSHV RTA utilizes the host E3 ubiquitin ligase complex RNF20/40 to drive lytic reactivation. J Virol 97:e0138923. https://doi.org/10.1128/jvi.01389-23
47. Yu Y, Wang SE, Hayward GS. 2005. The KSHV immediate-early transcription factor RTA encodes ubiquitin E3 ligase activity that targets IRF7 for proteosome-mediated degradation. Immunity 22:59–70. https://doi.org/10.1016/j.immuni.2004.11.011
48. Yang Z, Yan Z, Wood C. 2008. Kaposi's sarcoma-associated herpesvirus transactivator RTA promotes degradation of the repressors to regulate viral lytic replication. J Virol 82:3590–3603. https://doi.org/10.1128/JVI.02229-07
49. Gould F, Harrison SM, Hewitt EW, Whitehouse A. 2009. Kaposi's sarcoma-associated herpesvirus RTA promotes degradation of the Hey1 repressor protein through the ubiquitin proteasome pathway. J Virol 83:6727–6738. https://doi.org/10.1128/JVI.00351-09
50. Lan K, Kuppers DA, Verma SC, Robertson ES. 2004. Kaposi's sarcoma-associated herpesvirus-encoded latency-associated nuclear antigen inhibits lytic replication by targeting Rta: a potential mechanism for virus-mediated control of latency. J Virol 78:6585–6594. https://doi.org/10.1128/JVI.78.12.6585-6594.2004
51. Lan K, Kuppers DA, Robertson ES. 2005. Kaposi's sarcoma-associated herpesvirus reactivation is regulated by interaction of latency-associated nuclear antigen with recombination signal sequence-binding protein Jκ, the major downstream effector of the Notch signaling pathway. J Virol 79:3468–3478. https://doi.org/10.1128/JVI.79.6.3468-3478.2005
52. Gu F, Wang C, Wei F, Wang YY, Zhu Q, Ding L, Xu WJ, Zhu CX, Cai CK, Qian ZK, Yuan ZH, Robertson E, Cai QL. 2018. STAT6 degradation and ubiquitylated TRIML2 are essential for activation of human oncogenic herpesvirus. PLoS Pathog 14:e1007416. https://doi.org/10.1371/journal.ppat.1007416
53. Reid EG. 2011. Bortezomib-induced Epstein-Barr virus and Kaposi sarcoma herpesvirus lytic gene expression: oncolytic strategies. Curr Opin Oncol 23:482–487. https://doi.org/10.1097/CCO.0b013e3283499c37
54. Laurent-Rolle M, Morrison J, Rajsbaum R, Macleod JML, Pisanelli G, Pham A, Ayllon J, Miorin L, Martinez C, tenOever BR, García-Sastre A. 2014. The interferon signaling antagonist function of yellow fever virus NS5 protein is activated by type I interferon. Cell Host Microbe 16:314–327. https://doi.org/10.1016/j.chom.2014.07.015
55. Chang Y, Cesarman E, Pessin MS, Lee F, Culpepper J, Knowles DM, Moore PS. 1994. Identification of herpesvirus-like DNA sequences in AIDS-associated Kaposi's sarcoma. Science 266:1865–1869. https://doi.org/10.1126/science.7997879
56. Cesarman E, Chang Y, Moore PS, Said JW, Knowles DM. 1995. Kaposi's sarcoma-associated herpesvirus-like DNA sequences in AIDS-related body-cavity-based lymphomas. N Engl J Med 332:1186–1191. https://doi.org/10.1056/NEJM199505043321802
57. Wen KW, Damania B. 2010. Kaposi sarcoma-associated herpesvirus (KSHV): molecular biology and oncogenesis. Cancer Lett 289:140–150. https://doi.org/10.1016/j.canlet.2009.07.004
58. Martin JN, Osmond DH. 1999. Kaposi's sarcoma-associated herpesvirus and sexual transmission of cancer risk. Curr Opin Oncol 11:508–515. https://doi.org/10.1097/00001622-199911000-00013
59. Lukac DM, Kirshner JR, Ganem D. 1999. Transcriptional activation by the product of open reading frame 50 of Kaposi's sarcoma-associated herpesvirus is required for lytic viral reactivation in B cells. J Virol 73:9348–9361. https://doi.org/10.1128/JVI.73.11.9348-9361.1999
60. Overå KS, Garcia-Garcia J, Bhujabal Z, Jain A, Øvervatn A, Larsen KB, Deretic V, Johansen T, Lamark T, Sjøttem E. 2019. TRIM32, but not its muscular dystrophy-associated mutant, positively regulates and is targeted to autophagic degradation by p62/SQSTM1. J Cell Sci 132:jcs236596. https://doi.org/10.1242/jcs.236596
61. Ichimura T, Taoka M, Shoji I, Kato H, Sato T, Hatakeyama S, Isobe T, Hachiya N. 2013. 14-3-3 proteins sequester a pool of soluble TRIM32 ubiquitin ligase to repress autoubiquitylation and cytoplasmic body formation. J Cell Sci 126:2014–2026. https://doi.org/10.1242/jcs.122069

62. Xu X, Lai Y, Hua ZC. 2019. Apoptosis and apoptotic body: disease message and therapeutic target potentials. Biosci Rep 39:BSR20180992. https://doi.org/10.1042/BSR20180992
63. Sairanen T, Szepesi R, Karjalainen-Lindsberg ML, Saksi J, Paetau A, Lindsberg PJ. 2009. Neuronal caspase-3 and PARP-1 correlate differentially with apoptosis and necrosis in ischemic human stroke. Acta Neuropathol 118:541–552. https://doi.org/10.1007/s00401-009-0559-3
64. Brulois KF, Chang H, Lee ASY, Ensser A, Wong LY, Toth Z, Lee SH, Lee HR, Myoung J, Ganem D, Oh TK, Kim JF, Gao SJ, Jung JU. 2012. Construction and manipulation of a new Kaposi's sarcoma-associated herpesvirus bacterial artificial chromosome clone. J Virol 86:9708–9720. https://doi.org/10.1128/JVI.01019-12
65. Myoung J, Ganem D. 2011. Generation of a doxycycline-inducible KSHV producer cell line of endothelial origin: maintenance of tight latency with efficient reactivation upon induction. J Virol Methods 174:12–21. https://doi.org/10.1016/j.jviromet.2011.03.012
66. Jones T, Ye FC, Bedolla R, Huang YF, Meng J, Qian LW, Pan HY, Zhou FC, Moody R, Wagner B, Arar M, Gao SJ. 2012. Direct and efficient cellular transformation of primary rat mesenchymal precursor cells by KSHV. J Clin Invest 122:1076–1081. https://doi.org/10.1172/JCI58530
67. Zhu Q, Ding L, Zi Z, Gao S, Wang C, Wang Y, Zhu C, Yuan Z, Wei F, Cai Q. 2019. Viral-mediated AURKB cleavage promotes cell segregation and tumorigenesis. Cell Reports 26:3657–3671. https://doi.org/10.1016/j.celrep.2019.02.106
68. Brzozowska B, Gałecki M, Tartas A, Ginter J, Kaźmierczak U, Lundholm L. 2019. Freeware tool for analysing numbers and sizes of cell colonies. Radiat Environ Biophys 58:109–117. https://doi.org/10.1007/s00411-018-00772-z